Distance Distributions for Matérn Cluster Processes with Application to Network Performance Analysis

Jinchuan Tang, Gaojie Chen, Justin P. Coon, David E. Simmons
Department of Engineering Science
University of Oxford
Parks Road, Oxford, OX1 3PJ, UK.
{jinchuan.tang, gaojie.chen, justin.coon, david.simmons}@eng.ox.ac.uk.

***Abstract*—In this work, we analyze the distance statistics corresponding to points in a Matérn cluster (offspring points) and points that do not belong to that cluster (non-offspring points). We first derive the probability density function (PDF) of the distance between an offspring point and a non-offspring point of a Matérn cluster. We then formulate the probability generating functional based on this PDF. Since many wireless networks (e.g., device-to-device (D2D) networks and cognitive radio systems) exhibit device clustering, this formalism enables us to efficiently formulate and evaluate expressions that describe the interference statistics and connection probability in clustered networks. We validate our theoretical analysis with numerical simulations, and illustrate that traditional methods of evaluating similar performance metrics (based on point process statistics instead of distance statistics) are unsuitable for use in such complex scenarios.**

***Index Terms*—Interference, Matérn cluster process, distance probability density function, connection probability.**

I. Introduction

Recently, stochastic geometry has become a popular modeling tool for wireless communications networks. It has played a vital role in characterizing the system-level performance of wireless networks where the nodes are placed according to random spatial point patterns. These patterns describe the nature of wireless systems statistically. With spatial point processes, performance metrics such as connection and coverage probabilities are usually formed with tractable and computable expressions. Among the spatial point processes, the Poisson point process (PPP) is very popular. It has often been used to model the positions of wireless nodes such as base stations and mobile users, which are uniformly distributed in a plane. In [1] and [2], the authors presented tractable expressions for the coverage probability and average rate in the cellular downlink and uplink for both uniform and irregular network topologies. Dhillon et al [3] considered non-uniform user equipment (UE) distributions for random cellular networks. Di Renzo [4] modeled and analyzed multi-tier millimeter wave cellular networks with PPPs.

Many wireless networking paradigms exhibit node clustering behavior. Examples of networks where this phenomenon occurs include cognitive radio networks and D2D-enabled systems. Clustering can also be caused by geographical constraints or medium access control (MAC) protocols [5]. PPP models are not capable of representing wireless networks when node clustering occurs. For this reason, Poisson cluster processes (PCPs) have attracted attention in the community. In [6], the authors showed that a PCP could accurately model active cognitive users under an exclusion region setup. They also gave a comparative study of two types of PCPs: modified Thomas cluster processes and Matérn cluster processes. Ganti and Haenggi [5] studied interference and outage in clustered wireless ad hoc networks by exploiting Matérn cluster and modified Thomas cluster processes. The authors of [7] compared the performance differences between PPP-based and modified Thomas cluster node deployments in LTE two-tier femtocell networks.

The analyses noted above are based on point process formalisms. When considering inhomogeneous point processes in a plane, these approaches sometimes result in less tractable mathematical expressions that rely on multifold integration to obtain performance results. Often, standard mathematical software packages grind to a halt when trying to evaluate such complex expressions, thus rendering the impressive theoretical results less than immediately useful in determining practical system behavior.

An alternative to using a point process formalism is to invoke distance statistics. The distribution of distances between node locations is affiliated with the interference geometry and the performance of wireless networks [8]. It is, therefore, useful and important to derive the distribution of distances between nodes in PCPs. Notably, the authors of [9] realized the importance of distance statistics for analyzing modified Thomas clusters in D2D networks and were able to conduct a performance analysis based on the distance probability density function (PDF) in that scenario. Like the modified Thomas process, the Matérn cluster process is also important process for cluster analysis. In order to understand interference statistics, arising from a Matérn cluster of interferers, observed at any point on the plane, the distribution of the distance between an offspring point (of the cluster) and a non-offspring point must be known. To the best of our knowledge, no such result has been reported in the literature before now. Knowledge of this distance distribution would reduce the complexity of the associated performance analysis and reduce numerical computation time.

In this paper, we address the problem alluded to above. To this end, we first derive the distance PDF between an

offspring point of a Matérn cluster and a non-offspring point relative to the same cluster. We then provide a discussion of the corresponding probability generating functional (PGFL) based on this distance distribution. We also analyze the distance PDF between two offspring points in a Matérn cluster as well as the interference statistics and the connection probability for a Matérn clustered network. The analysis and simulations show that by using the distance statistics, the mathematical expressions in the analysis become tractable and computable.

The rest of the paper is organized as follows. Section II begins with the discussion of the definition of a Matérn cluster process, follows with a theorem on the new distance PDF noted above, and ends by addressing the PGFL based on the distance PDF. Section III focuses on a special case study that exhibits the usefulness of the distance PDF in characterizing interference and the connection probability for two devices. Section IV documents a comparison of theoretical and simulation results. Section V concludes the paper.

II. Distance distribution analysis

A. Matérn cluster process

In the Matérn cluster process, the distribution of parents on two-dimensional space $\mathbb{R}^2$ is a homogeneous PPP (HPPP) $\Phi_o = (N, X_o)$ with intensity λ_o. A realization of an HPPP on this space has an infinite number points, but is finite on any bounded window with probability tending to one. For a given observation window (Fig. 1), the HPPP describes that parents inside obey a Poisson distribution in number and uniform distribution in location. The offspring points of a parent are retrieved by replacing the parent with a number of points obeying a Poisson distribution, then distributing the offspring points uniformly inside a disk-shaped cluster $b(\mathbf{x}_o, R)$ centered at parent $\mathbf{x}_o$ with radius R. The PDF of the offspring points inside this cluster is given by

$$f(\mathbf{u}-\mathbf{x}_o) = \frac{1}{\pi R^2}, \text{ for } r = \|\mathbf{u}-\mathbf{x}_o\| \le R. \tag{1}$$

From now on, each cluster consists only of offspring points. Any point which does not belong to a cluster is called a non-offspring point of that cluster. The cluster origins are distributed independently. Thus it is possible that an offspring point $\mathbf{u}_1$ of cluster I is within the radius of cluster II, but $\mathbf{u}_1$ is a non-offspring point of cluster II.

B. A new distance distribution

Random network performance metrics such as capacity and connection probability are related to the distances between the nodes. By providing the distance PDF, the complexity of the analysis of these metrics is shown to decrease in [9]. For two offspring points belonging to a Matérn cluster, the PDF of their distance D is given by [10]

$$f_D(d) = \frac{4d}{\pi R^2}\left(\arccos\left(\frac{d}{2R}\right) - \frac{d}{2R}\sqrt{1-\left(\frac{d}{2R}\right)^2}\right), \tag{2}$$

where $0 \le d \le 2R$.

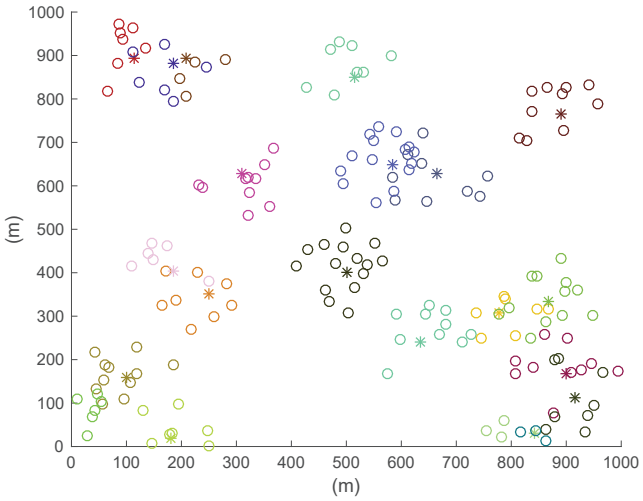

Fig. 1. The Matérn clusters where $*$ denotes the parents and $\circ$ denotes the offspring points. The parent density is 13 points per km^2. $R = 100$ m, each cluster is set to have an average of 9 offspring points.

Interestingly, the distance distribution between an offspring point and a non-offspring point of the same cluster has not been reported in the literature. To solve this problem, traditional methods described in [5], [6] reformulate the analysis by forming distance relationships based on points and the point PDF given by (1). This formulation is deficient in terms of the analytical complexity and computation time of the resulting mathematical expressions because the number of integrals is twice the number of integrals encountered when the problem is formulated using distance statistics (in two-dimensional space). Observing that the distance distribution is of great importance to the analysis of clusters in wireless networks, we give the following theorem, which provides the distance PDF between an offspring point and a non-offspring point of a Matérn cluster.

Theorem 1. *Let R_d be a random variable representing the distance between an offspring point and a non-offspring point of a Matérn cluster with radius R. Conditioning on the distance R_y from the cluster origin to the non-offspring point, the PDF of R_d is given by*

$$f_{R_d}(r_d \mid R_y) = \frac{c(r_d)}{\pi R^2}, \tag{3}$$

where for $R_y > R$,

$$c(r_d) = \begin{cases} c_1(r_d), & r_d \in [R_y - R, R_y + R], \\ 0, & \text{otherwise}; \end{cases}$$
$$c_1(r_d) = 2r_d \arcsin \frac{\sqrt{4R_y^2 r_d^2 - (R_y^2 - R^2 + r_d^2)^2}}{2R_y r_d}; \tag{4}$$

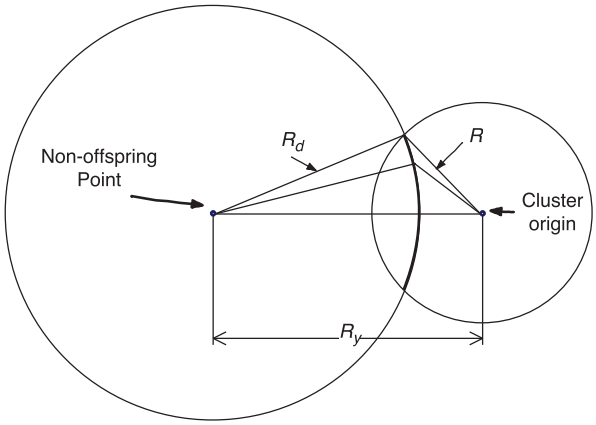

Fig. 2. The non-offspring point is outside the cluster, and a cluster encloses the arc of a circle.

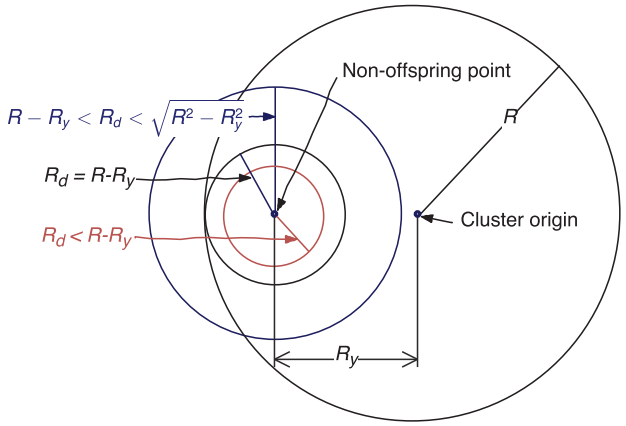

Fig. 3. The non-offspring point is inside the cluster, and a cluster encloses an arc or a circle where $R_d < \sqrt{R^2 - R_y^2}$.

otherwise,

$$c(r_d) = \begin{cases} 2\pi r_d, & r_d \leq R - R_y, \\ 2\pi r_d - c_1(r_d), & R - R_y < r_d \leq \sqrt{R^2 - R_y^2}, \\ c_1(r_d), & \sqrt{R^2 - R_y^2} < r_d \leq R + R_y, \\ 0, & \text{otherwise.} \end{cases} \tag{5}$$

Proof: When $R_y > R$, the non-offspring point is outside the Matérn cluster. The possible locations of the offspring point that have the same distance to the non-offspring point are on the circular arc of a circle that is enclosed by the cluster as shown in Fig. 2. When R_d is increasing from $R_y - R$ to $R_y + R$, the cluster can be filled with an infinite number of non-overlapping arcs, and each arc represents a class of points that have the same distance to the non-offspring point. Hence by calculating the arc length with (4), the corresponding density for R_d is achieved in (3).

When $0 < R_y \leq R$, the non-offspring point is inside the Matérn cluster. The possible locations of the offspring point that have the same distance to a non-offspring point could be on: (i) the circle centered at the non-offspring point when $R_d \leq R - R_y$ as depicted in Fig. 3; (ii) the circular arc of a circle with radius R_d that is enclosed by the cluster with radius R as seen in Figs. 3 and 4. The former is the perimeter of a circle with radius R_d, which is the first case of (5). The latter belongs to the second and third cases of (5). $\sqrt{R^2 - R_y^2}$ is the boundary to decide if the circular arc enclosed by the cluster is the major or minor arc of a circle with radius R_d.

When $R_y = 0$, the non-offspring point is overlapping with the cluster origin. The possible locations of the offspring point that have the same distance to the non-offspring point form a circle with radius R_d centered at the cluster origin. It belongs to the first case in (5). Thus we conclude our proof. ∎

Fig. 5 shows two examples of Theorem 1. Both examples are given the same cluster radius R but different values of R_y to demonstrate both (4) and (5). The solid line shows that (4) offers a smooth concave curve while the dashed line shows signs of transitions in (5). The tip and the inflection point on the dashed line are the transition points from case one to two and case two to three in (5), respectively. The simulation results have shown in the examples a good match to the theoretical values.

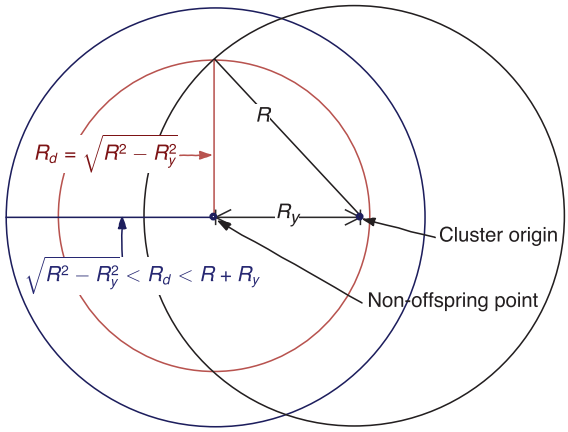

Fig. 4. The non-offspring point is inside the cluster, and a cluster encloses an arc or a circle where $R_d > \sqrt{R^2 - R_y^2}$.

C. Probability generating functional (PGFL)

A Matérn cluster process is a type of Neyman-Scott process, hence it follows the definition of the probability generating functional (PGFL) for the Neyman-Scott processes. For a given function $g : \mathbb{R}^2 \to [0, 1]$ and $\int_{\mathbb{R}^2} |1 - g(\mathbf{x})| \mathrm{d}\mathbf{x} < \infty$, where $\mathbf{x} = (x_1, x_2)$ denotes the Cartesian coordinate of a point in the two-dimensional plane, the PGFL of a Neyman-Scott process Φ is given by [11]

$$\mathbb{G}_\Phi(g) = \mathbb{E}_\Phi \left[\prod_{\mathbf{x} \in \Phi} g(\mathbf{x}) \right]$$
$$= \exp \left\{ \lambda \int_0^{2\pi} \int_0^{\infty} \left[\eta \left(\int_{\mathbb{R}^2} g(\mathbf{x} + \mathbf{s_1}) f(\mathbf{x}) \mathrm{d}\mathbf{x} \right) - 1 \right] r \mathrm{d}r \mathrm{d}\theta \right\}, \tag{6}$$

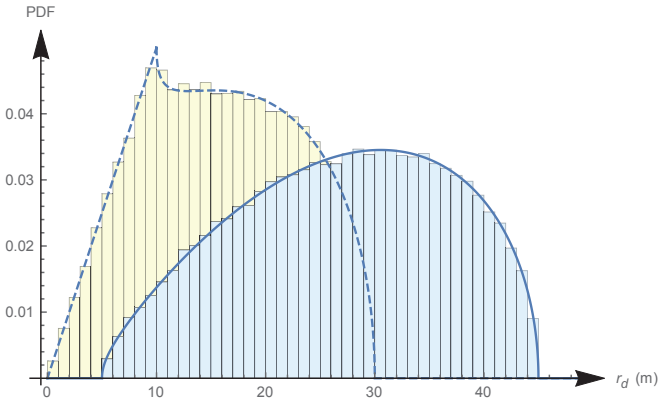

Fig. 5. The plot of (3) where the dashed line represents the PDF given by $R_y = 10$ m and $R = 20$ m, while the solid line represents the PDF given by $R_y = 25$ m and $R = 20$ m. The bins represent the simulation results for both PDFs.

where $\mathbf{s_1} = (r\cos(\theta), r\sin(\theta))$, $\eta(z)$ is the moment-generating function of a Poisson random variable which describes the distribution of the number of offspring points in a cluster, and $f(\mathbf{x})$ is the PDF of the points in the cluster, which equals (1) for a Matérn cluster process with radius R.

Noticing that $R_y = r$ and having the distance PDF given by Theorem 1, we see that if $g(\mathbf{x})$ is equal to a distance function $g_1(||\mathbf{x}||)$, the PGFL is given by

$$\mathbb{G}_\Phi(g_1) = \exp\left\{2\pi\lambda \int_0^\infty \left[\eta\left(\int_{\mathbb{D}} g_1(x) f_{R_d}(x \mid r)\mathrm{d}x\right) - 1\right] r\mathrm{d}r\right\}, \tag{7}$$

where $\mathbb{D} = [[r-R]^+, r+R]$ is the domain for the distance PDF in Theorem 1, and $[r-R]^+ = \max(0, r-R)$. Notably, the number of integrals is reduced from 4 integrals in (6) to 2 integrals in (7).

III. Applications

To understand how to use the distance statistics for network performance analysis, we provide a case study.

A. System model

To exploit the distance PDFs for cluster interference analysis, we focus on a special case study where the simultaneously active transmitting nodes, which use the same channel resource, are distributed according to Matérn cluster processes. We assume that the intensity of the cluster centers is λ_o, the mean number of the transmitting nodes in a cluster is $\overline{m}$ and the corresponding receiving nodes are uniformly distributed in the clusters. Therefore, a typical receiving node inside a cluster experiences interference from the undesired transmitting nodes, which are active simultaneously. To simplify the analysis, we choose the path loss model[1] $l(\|\mathbf{x}-\mathbf{y}\|) = (\lambda/4\pi)^2\|\mathbf{x}-\mathbf{y}\|^{-\alpha}$, which is given by [13], where λ represents the carrier wavelength and $\|\mathbf{x}-\mathbf{y}\|$ is the distance between a node at point $\mathbf{x}$ and a node at point $\mathbf{y}$. Without loss of generality, we assume that the fading of each channel is Rayleigh distributed. The gain due to coding, transmitting antenna and receiving antenna is G_e. Hence, $(\lambda/4\pi)^2 l(\|\mathbf{x}-\mathbf{y}\|)$ is the link gain. The power of a typical transmitting node is P_d.

[1]Other path-loss models such as empirically based models and log-normal shadowing [12] are also applicable to our analysis, but they are out of the scope of this paper.

B. Interference analysis

1) Interference analysis in general: The total interference power measured at a receiving node at point $\mathbf{x}$ is given by

$$I(\mathbf{x}) = \sum_{\mathbf{y}\in\Phi} P_{r_\mathbf{y}}(\mathbf{x}) = \sum_{\mathbf{y}\in\Phi} G_e \ell(\|\mathbf{x}-\mathbf{y}\|)|h_{\mathbf{xy}}|^2 P_d, \tag{8}$$

where Φ is a point process, which consists of simultaneously active transmitting nodes, and $P_{r_\mathbf{y}}(\mathbf{x})$ is the interference received at point $\mathbf{x}$ from one such node at point $\mathbf{y}$.

Considering the interference as a shot noise process and identifying the fading terms $h_{\mathbf{xy}}$ as independent and identically distributed (i.i.d.) fading h, the Laplace transform of the interference is defined as [14]

$$\begin{aligned}\mathcal{L}_I(s) &= \mathbb{E}_{\Phi,h}[\exp(-sI(\mathbf{x}))] \\ &= \mathbb{E}_\Phi\left[\prod_{\mathbf{y}\in\Phi} \frac{1}{1+sG_e\ell(\|\mathbf{x}-\mathbf{y}\|)P_d}\right].\end{aligned} \tag{9}$$

In our system, Φ causes two independent types of interference: *intra-cluster* and *inter-cluster* interference. Given a receiving node inside a cluster, the former describes the interference to the receiving node coming from the simultaneously active transmitting nodes in the same cluster, while the latter accounts for the interference coming from the simultaneously active transmitting nodes from other clusters.

The following two subsections study the intra-cluster and inter-cluster interference analysis respectively. Each subsection begins with the traditional analysis based on point coordinates and ends up with the proposed analysis based on distance.

2) Intra-cluster interference:

a) Analysis based on point coordinates: Assuming that a typical receiver is at the origin and its cluster is centered at point $\mathbf{c}$, the Laplace transform of the intra-cluster interference based on point coordinates and the point distribution (1) is given by

$$\mathcal{L}_I^{intra}(s) = \int_{\mathbb{R}^2} \mathcal{L}_I^{intra}(s \mid \mathbf{c})\, f(\mathbf{c})\mathrm{d}\mathbf{c}, \tag{10}$$

where

$$\mathcal{L}_I^{intra}(s \mid \mathbf{c}) = \exp\left\{-(\overline{m}-1)\int_{\mathbb{R}^2} \frac{g(\mathbf{a}+\mathbf{c})}{s^{-1}+g(\mathbf{a}+\mathbf{c})} f(\mathbf{a})\mathrm{d}\mathbf{a}\right\}, \tag{11}$$

with $g(\mathbf{x}) = G_e P_d \ell(\|\mathbf{x}\|)$. As observed from above, the Laplace transform of all the interferers in a cluster can be characterized by a typical interferer with an offset $\mathbf{a}$ from a cluster center $\mathbf{c}$. $\mathcal{L}_I^{intra}(s \mid \mathbf{c})$ is the Laplace transform of intra-cluster interference conditioning on the cluster center $\mathbf{c}$.

By marginalizing over the possible locations of the cluster center $\mathbf{c}$, $\mathcal{L}_I^{intra}(s)$ is retrieved.

b) Analysis based on distance: The PDF of distance D between the receiving node and interferer, which are independently and uniformly distributed in a circular area with radius R is given by (2); hence the distance version of intra-cluster interference in the PCP is written as

$$\mathcal{L}_I^{intra}(s) = \exp\left(-(\overline{m}-1)\int_0^{2R} \frac{g_1(x)}{s^{-1}+g_1(x)} f_D(x)\mathrm{d}x\right), \tag{12}$$

where $g_1(x) = G_e P_d \ell(x)$.

3) Inter-cluster interference:

a) Analysis based on point coordinates: The Laplace transform of inter-cluster interference based on point distributions is given by

$$\mathcal{L}_I^{inter}(s) = \exp\left(-\lambda_o \int_{\mathbb{R}^2} [1-\xi_1(s,\mathbf{c})]\mathrm{d}\mathbf{c}\right). \tag{13}$$

where

$$\xi_1(s,\mathbf{c}) = \exp\left\{-\overline{m}\int_{\mathbb{R}^2} \frac{g(\mathbf{a}+\mathbf{c})}{s^{-1}+g(\mathbf{a}+\mathbf{c})} f(\mathbf{a})\mathrm{d}\mathbf{a}\right\}. \tag{14}$$

b) Analysis based on distance: Applying (7), the Laplace transform of inter-cluster interference based on the distance distribution is written as

$$\mathcal{L}_I^{inter}(s) = \exp\left(-2\pi\lambda_o \int_0^{\infty} [1-\xi_2(s,v)]\, v\mathrm{d}v\right), \tag{15}$$

where

$$\xi_2(s,v) = \exp\left\{-\overline{m}\int_{[v-R]^+}^{v+R} \frac{g_1(x)}{s^{-1}+g_1(x)} f_{R_d}(x \mid v)\mathrm{d}x\right\}. \tag{16}$$

As a result of the above discussion, we have successfully built up the methods for interference analysis based on the distribution of distance.

C. Connection probability analysis

The connection probability of a link is the likelihood that the actual SINR of the link is higher than a predetermined threshold $\beta = 2^t - 1$. The parameter $t = R_b/B$ is the predefined link spectrum efficiency for a node, R_b is the target rate of the link in bit/s, and B is the transmission bandwidth.

Giving the distance d between a typical transmitting node and receiving node and considering that the noise and interference are independent of each other [15], the connection probability of the typical transmitting node is given by

$$\begin{aligned} p(d) &= \exp\left(-\frac{\beta N_0}{g_1(d)}\right)\mathcal{L}_I\left(\frac{\beta}{g_1(d)}\right) \\ &= \exp\left(-\frac{\beta N_0}{g_1(d)}\right)\mathcal{L}_I^{intra}\left(\frac{\beta}{g_1(d)}\right)\mathcal{L}_I^{inter}\left(\frac{\beta}{g_1(d)}\right), \end{aligned} \tag{17}$$

where N_0 is the thermal noise power at the receiving node, and the final term is because the intra-cluster interference and inter-cluster interference are also independent. Eqs. (12) and (15) are chosen respectively for (17). Because the transmitting node and receiving node are uniformly distributed in the cluster, the connection probability of a typical receiving node in a Matérn cluster is given by

$$p = \int_0^{2R} p(r_d) f_D(r_d)\mathrm{d}r_d. \tag{18}$$

It is worth noting that (18) is easy to solve numerically with software such as Matlab and Mathematica. The point-based analysis, on the other hand, has to condition on the position of the cluster center with $\mathcal{L}_I^{intra}(s \mid \mathbf{c})$ because the transmitting node and the intra-cluster interferers share the same cluster. As a result of this, additional averaging (integration) is introduced into the formulation. Hence, the distance-based analysis helps to reduce the complexity and dimension of the problem so that the expressions become more tractable.

TABLE I
SYSTEM PARAMETERS.

Parameter	value
Bounded area	4 km × 4 km
Observing window area A	2 km × 2 km
Transmission bandwidth B	20 MHz
Duplex mode	Half duplex
Thermal noise power density	-174 dBm/Hz
Cluster radius R	12.5 m, 50 m, 100 m
Transmitting power level P_d	23 dBm
Coding gain	0 dB
Transmitting antenna gain	0 dBi
Receiving antenna gain	0 dBi
Transceiver noise figure	9 dB
Link spectrum efficiency	0.05 bps/Hz
Carrier frequency	2 GHz
Pathloss exponent	2.7
Simulation iterations	10^4

IV. SIMULATION RESULTS

In this section, we provide simulation results to validate the method detailed above. The parameters used in the simulation are given in Table I. The simulation results are obtained by averaging over 10^4 independent Monte Carlo trials. To combat boundary effects, we use the measurements recorded in an observation window with area A centered in a bounded area. The average number of clusters in the observation window is $A \times \lambda_o$.

Fig. 6 shows that for a given average number of clusters, the connection probability of a network node decreases as the average number of transmitting nodes in each cluster $\overline{m}$ increases. The numerical integrations of (18) for each point were computed using Mathematica with default working precision on an Intel Core i7-4790 PC with 16 GB memory for approximately 14.7 minutes. Meanwhile, traditional point-based analysis gave no result after several hours running on the computer.

Fig. 7 illustrates that the average connection probability of a typical network node decreases drastically as the cluster density λ_o increases. For a given average number of nodes $\overline{m}$ within the cluster, the larger the radius of the cluster, the smaller average connection probability the system will have. It

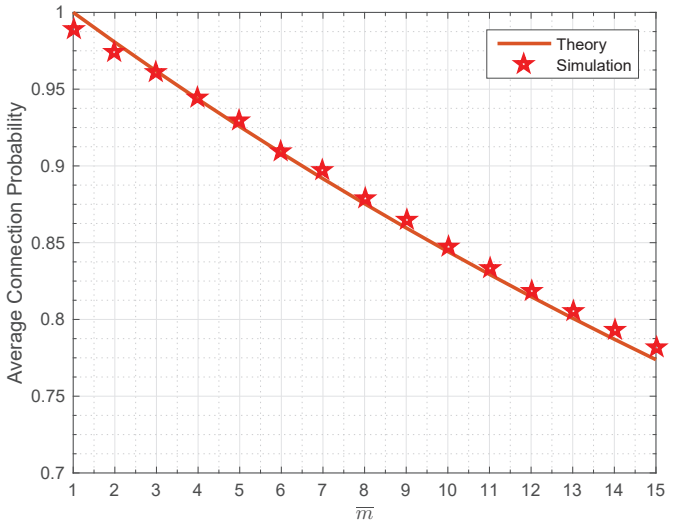

Fig. 6. The average connection probability of a typical node in the Matérn cluster of the network vs. an average of $\overline{m}$ transmitting nodes inside each cluster. λ_o is 0.5 points per km^2, and $R = 12.5$ m. The average number of clusters in the observing window is $A \times \lambda_o = 2$.

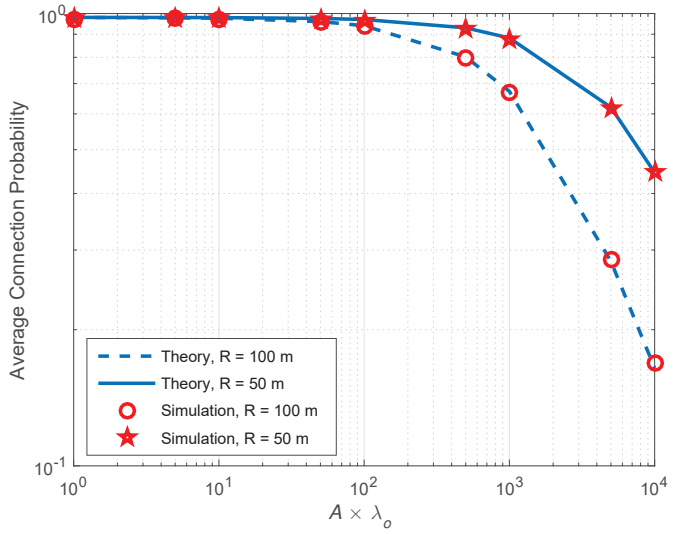

Fig. 7. The average connection probability of a typical node vs. the average number of clusters in the observing window: $A \times \lambda_o$. The average number of transmitting nodes in a cluster is $\overline{m} = 2$.

is because the radius is increasing so that the transmitting and receiving nodes have a larger separation on average and the interferers are also closer to the receiving node (on average).

V. Conclusion

In this paper, we formulated the distance PDF between an offspring point and a non-offspring point of a Matérn cluster. Based on this, we have characterized the PGFL, interference statistics and connection probability of a typical network node. By doing so, the number of integrals is halved compared to the traditional point-based method. Our method achieves more tractable and computable expressions. Therefore, the proposed methods will facilitate performance analysis for wireless networks such as cognitive radio systems and D2D communications for 5G and beyond.

Acknowledgment

The authors wish to acknowledge the support of EPSRC grant EP/N002350/1.

References

[1] J. G. Andrews, F. Baccelli, and R. K. Ganti, "A tractable approach to coverage and rate in cellular networks," *IEEE Trans. Commun.*, vol. 59, no. 11, pp. 3122–3134, Nov. 2011.

[2] T. D. Novlan, H. S. Dhillon, and J. G. Andrews, "Analytical modeling of uplink cellular networks," *IEEE Trans. Wireless Commun.*, vol. 12, no. 6, pp. 2669–2679, Jun. 2013.

[3] H. S. Dhillon, R. K. Ganti, and J. G. Andrews, "Modeling non-uniform UE distributions in downlink cellular networks," *IEEE Wireless Commun. Lett.*, vol. 2, no. 3, pp. 339–342, Jun. 2013.

[4] M. Di Renzo, "Stochastic geometry modeling and analysis of multi-tier millimeter wave cellular networks," *IEEE Trans. Wireless Commun.*, vol. 14, no. 9, pp. 5038–5057, Sep. 2015.

[5] R. K. Ganti and M. Haenggi, "Interference and outage in clustered wireless ad hoc networks," *IEEE Trans. Info. Theory*, vol. 55, no. 9, pp. 4067–4086, Sep. 2009.

[6] C. h. Lee and M. Haenggi, "Interference and outage in Poisson cognitive networks," *IEEE Trans. Wireless Commun.*, vol. 11, no. 4, pp. 1392–1401, Apr. 2012.

[7] Z. Jakó and G. Jeney, "Outage probability in Poisson-cluster-based LTE two-tier femtocell networks," *Wireless Commun. Mob. Comput.*, vol. 15, no. 18, pp. 2179–2190, Jun. 2015.

[8] F. Voss, C. Gloaguen, F. Fleischer, and V. Schmidt, "Distributional properties of Euclidean distances in wireless networks involving road systems," *IEEE J. Sel. Areas Commun*, vol. 27, no. 7, pp. 1047–1055, Sep. 2009.

[9] M. Afshang, H. Dhillon, and P. Chong, "Modeling and performance analysis of clustered device-to-device networks," *IEEE Trans. Wireless Commun.*, vol. 15, no. 7, pp. 4957–4972, Jul. 2016.

[10] H. C. Tuckwell, *Elementary applications of probability theory*. London, UK: Chapman & Hall, 1995.

[11] R. K. Ganti and M. Haenggi, "Interference and outage in clustered wireless ad hoc networks," *IEEE Trans. Info. Theory*, vol. 55, no. 9, pp. 4067–4086, Sep. 2009.

[12] B. Black, P. DiPiazza, B. Ferguson, D. Voltmer, and F. Berry, *Introduction to Wireless Systems*, 1st ed. Upper Saddle River, NJ: Prentice Hall Press, 2008.

[13] E. McCune, *Practical digital wireless signals*, ser. The Cambridge RF and Microwave Engineering Series. Cambridge, UK: Cambridge Uni. press, 2013.

[14] C.-h. Lee and M. Haenggi, "Interference and outage in Poisson cognitive networks," *IEEE Trans. Wireless Commun.*, vol. 11, no. 4, pp. 1392–1401, Apr. 2012.

[15] M. Haenggi and R. K. Ganti, "Interference in large wireless networks," *Found. Trends Netw.*, vol. 3, no. 2, pp. 127–248, Feb. 2009.